Table S1: Observed and expected numbers of *Pf4-Cre;Pdgfb*$^{fl/fl}$ embryos at different developmental stages. Embryos were harvested at three different gestational stages: embryonic day (E) 14.5, E15.5 and E17.5. Despite the deletion of *Pdgfb* from platelets, embryos were born close to the expected amounts.

Developmental stage	Total amount of embryos	Expected amount of *Pf4-Cre;Pdgfb*$^{fl/fl}$ embryos	Seen amount of *Pf4-Cre;Pdgfb*$^{fl/fl}$ embryos
Progeny from *Pf4-Cre;Pdgfb*$^{fl/wt}$ x *Pdgfb*$^{fl/fl}$ cross			
E14.5	10	2.5	2
Progeny from *Pf4-Cre;Pdgfb*$^{fl/wt}$ x *Pdgfb*$^{fl/wt}$ cross			
E15.5	19	2.4	2
E17.5	10	1.3	2

Supplementary Figure 1

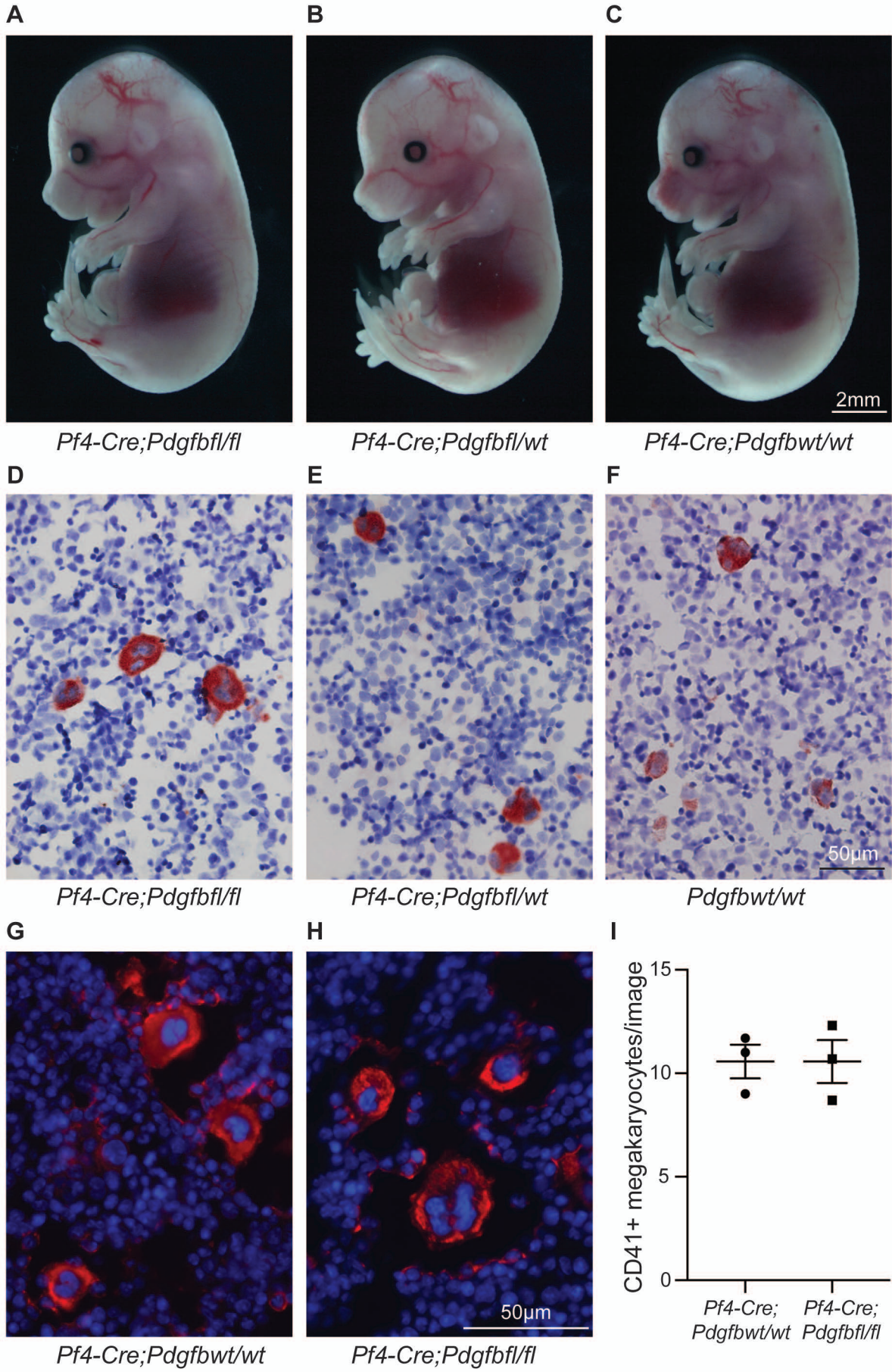

Supplementary Figure 2

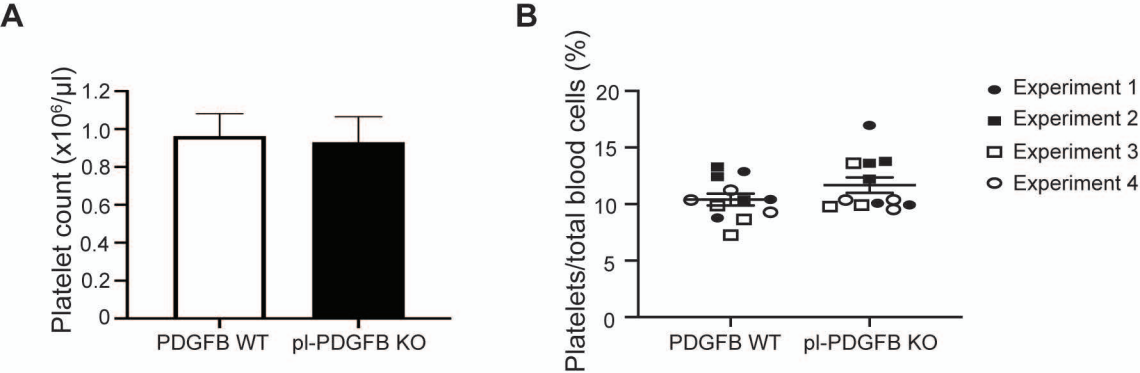

Supplementary Figure 3

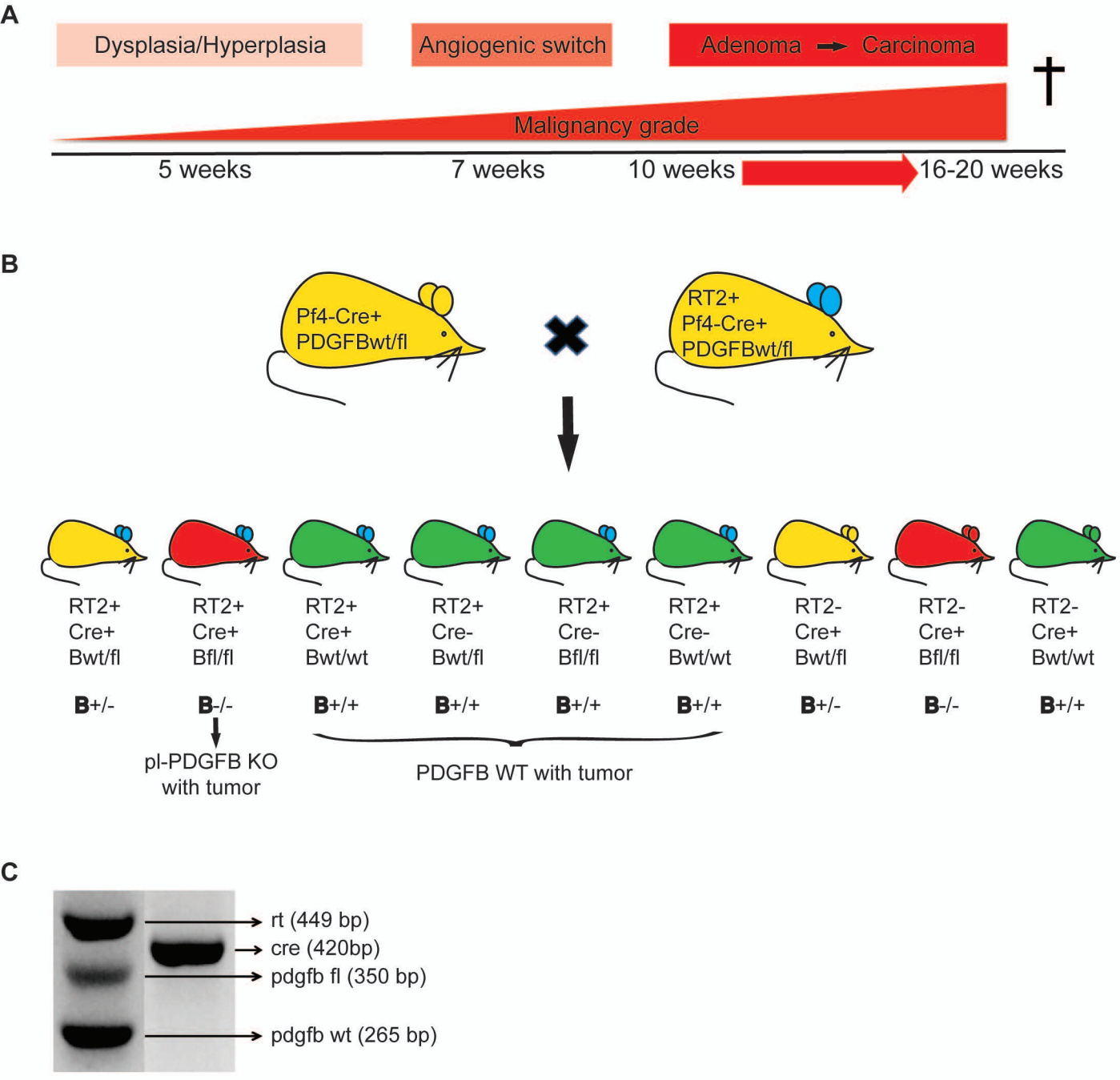

Supplementary Figure 4

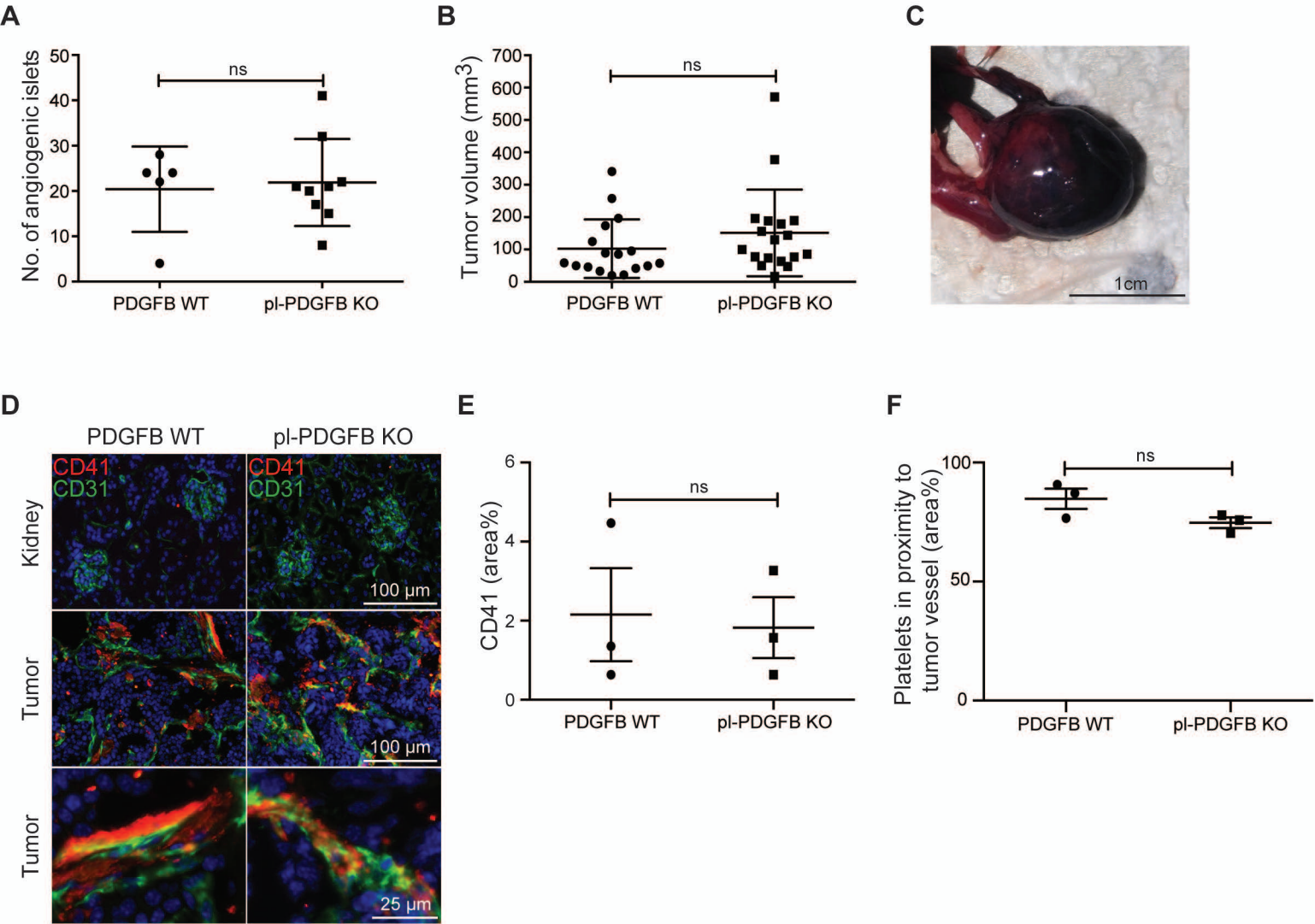

Supplementary Figure 5

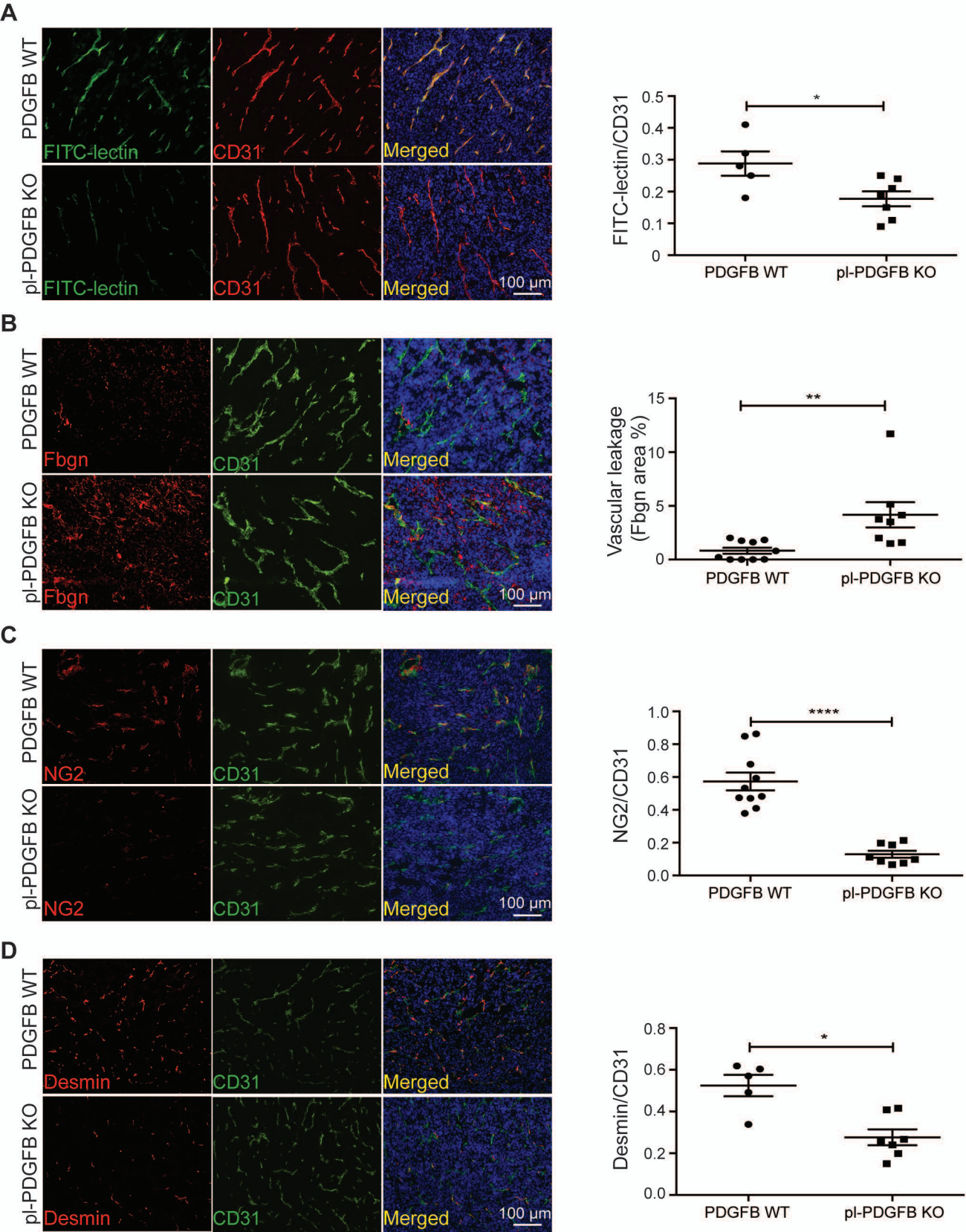

Supplementary Figure 6

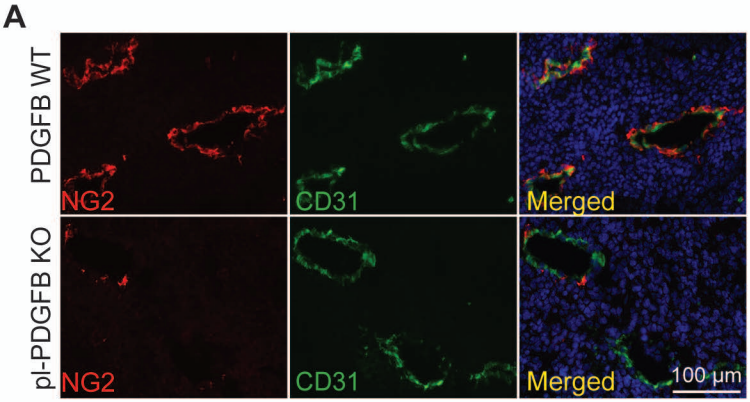

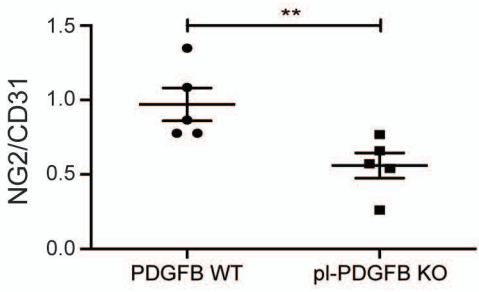

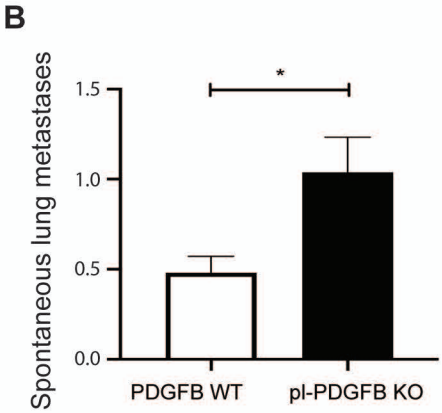

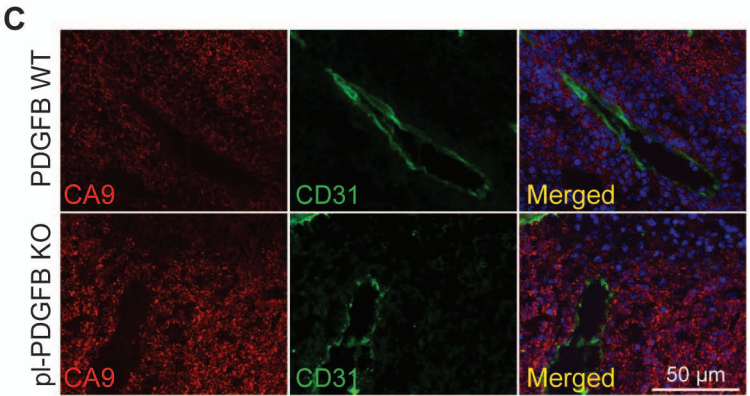

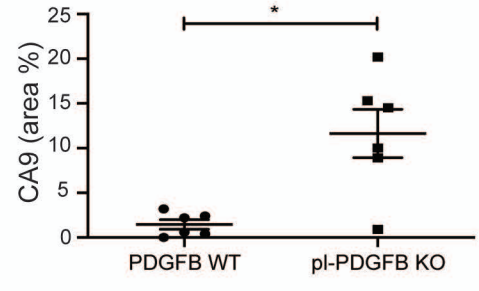

Supplementary Figure 7

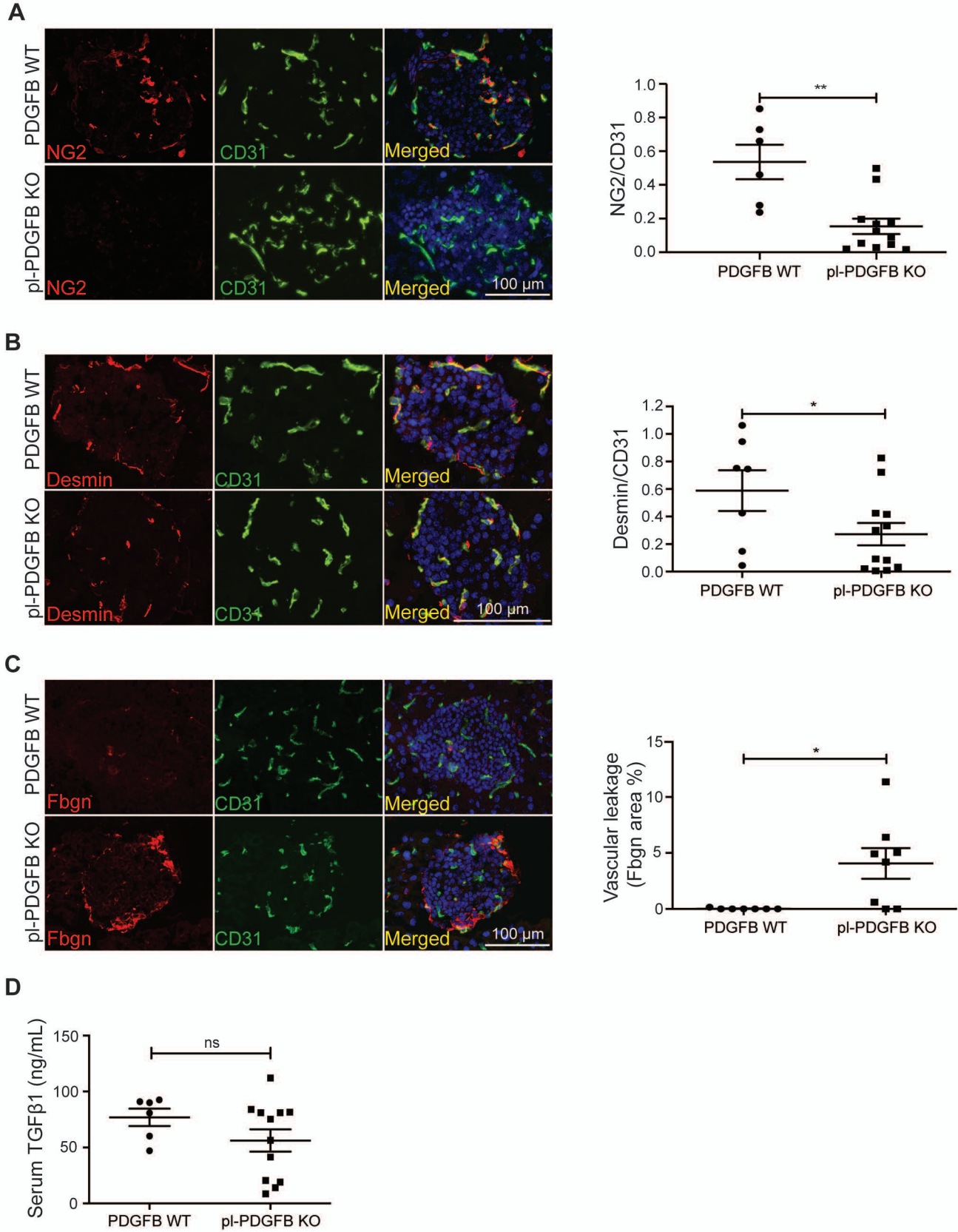

Supplementary Figure 8

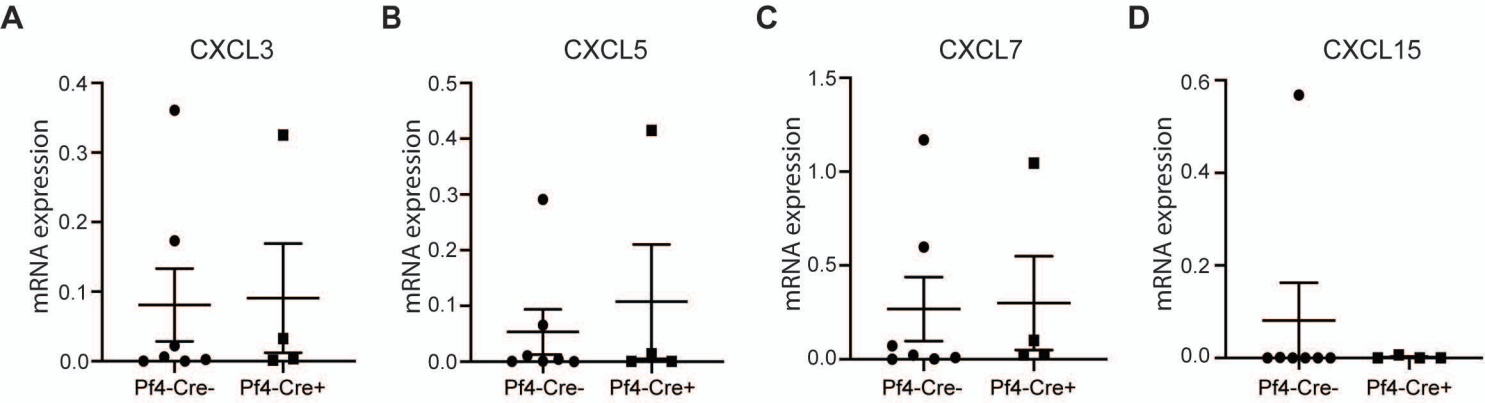

Supplementary figure legends

Figure S1: Platelet-specific PDGFB knockout embryos display no obvious abnormalities. Macroscopic appearance of freshly dissected (A) *Pf4-Cre;Pdgfb*$^{fl/fl}$, (B) *Pf4-Cre;Pdgfb*$^{fl/wt}$ and (C) *Pf4-Cre;Pdgfb*$^{wt/wt}$ embryos at embryonic day 15.5 (E15.5). CD41-positive megakaryocytes (red) in (D) *Pf4-Cre;Pdgfb*$^{fl/fl}$, (E) *Pf4-Cre;Pdgfb*$^{fl/wt}$ and (F) *Pdgfb*$^{wt/wt}$ embryos at E15.5. (G-H) Immunostaining and (I) quantification of CD41-positive megakaryocytes in bone marrow from adult *Pf4-Cre and Pf4-Cre;Pdgfb*$^{fl/fl}$ mice (n=3/group, P>0.9999). Error bars in the graph represent the standard error of mean (SEM).

Figure S2: Platelet counts and proportion in peripheral blood from WT and pl-PDGFB KO mice. (A) Platelet counts (n=3/group, P=0.5000) and (B) proportion of total blood cells (n=12/group, P=0.2476) in peripheral blood from pl-PDGFB KO and WT mice. Error bars in the graphs represent the standard error of mean (SEM).

Figure S3: Generation of RIP1-Tag2 mice lacking PDGFB in platelets. (A) Schematic illustration showing the step-wise tumor progression in RIP1-Tag2 mice. (B) Illustration describing the cross-breeding scheme to generate RIP1-Tag2 mice with platelet-specific PDGFB ablation. Green mice are PDGFB WT, yellow mice are pl-PDGFB HET and red mice pl-PDGFB KO. Blue ears indicate RT2-positive. (C) Genotyping was performed for the wild-type and floxed *Pdgfb* alleles, as well as for *Cre*, and generated PCR products of sizes 265 bp, 350 bp and 420 bp, respectively. The RT2 transgene generated a PCR product of 449 bp and due to the similar size of the *Cre* band, *Cre* was analyzed separately.

Figure S4: Lack of platelet PDGFB does not affect the angiogenic switch or tumor growth in RT2 mice. (A) The number of angiogenic islets were analyzed in seven-week old

WT and pl-PDGFB KO mice (WT n=5; KO n=9, *P*=0.5470). (B) Tumor volumes were analyzed in 14-week old WT and pl-PDGFB KO mice (WT n=17; KO n=18, *P*=0.1528). (C) Example of a blood-filled cyst found in association with the tumor tissue in a proportion of the pl-PDGFB KO mice. (D) Immunostaining for blood vessels (CD31) and platelets (CD41) in kidney (top row) from RT2-negative mice and tumor tissue (middle row and lower row, magnification) from 14-week old WT and pl-PDGFB KO mice. (E) Quantification of total CD41+ platelets in tumor tissue (n=3/group, *P*>0.9999) and (F) the proportion of CD41+ platelets in close proximity (7 μm) to tumor vessels (perivascular) (n=3/group, *P*=0.2000). Error bars in the graphs represent the standard error of mean (SEM).

Figure S5: Tumor vessels in MC38 colon carcinoma in mice with platelet-specific PDGFB ablation have impaired function and decreased pericyte coverage. Sections of MC38 tumor tissue from FITC-lectin perfused WT and pl-PDGFB KO mice were immunostained for CD31 and analyzed for (A) the proportion of FITC-lectin perfused vessels (FITC/CD31 ratio) (WT n=5; KO n=7, *P*=0. 0303), (B) the amount of extravasated fibrinogen (Fbgn) as a read out for vascular leakage (WT n=10; KO n=8, *P*=0.0043) and the extent of (C) NG2+ (WT n=10; KO n=8, *P*<0.0001) and (D) desmin+ (WT n=5; KO n=7, *P*=0.0101) pericyte coverage. Error bars in the graphs represent the standard error of mean (SEM).

Figure S6: Increased spontaneous lung metastasis in mice with platelet-specific PDGFB ablation in the HCmel12 melanoma model. WT and pl-PDGFB KO mice were subcutaneously injected with HCmel12 cells and followed for 24 days. (A) Immunostaining for blood vessels (CD31) and pericytes (NG2) in HCmel12 tumor sections and quantification of the extent of pericyte coverage in tumor vessels (n=5/group, *P*=0.0079). (B) Quantification of spontaneous lung metastasis in WT and pl-PDGFB KO mice injected with HCmel12 cells

by H&E staining of lung tissue sections obtained from four distinct levels. The graph represents the average number of metastases/lung section, in mice with metastasis (WT n=9; KO n=15, *P*=0.0483). (C) Immunostaining for the hypoxia-inducible target carbonic anhydrase 9 (CA9) in HCmel12 tumor sections and quantification of the expression level (n=6/group, *P*=0.0152). Error bars in the graph represent the standard error of mean (SEM).

Figure S7: Reduced pericyte coverage already in pre-tumorigenic tissue in mice lacking PDGFB in platelets. Immunostaining for CD31 and (A) NG2 (WT n=6; KO n=12, *P*=0.0020), (B) desmin (WT n=7; KO n=12, *P*=0.0449) and (C) fibrinogen (Fbgn) (WT n=7; KO n=8, *P*=0.0107) in pre-tumorigenic tissue from seven-week old WT and pl-PDGFB KO RT2-positive mice. (D) TGFβ1 concentration in serum from WT and pl-PDGFB KO mice was determined using ELISA (WT n=6; KO n=12, *P*=0.1797). Error bars in the graphs represent the standard error of mean (SEM).

Figure S8: Expression of Cxcl3, Cxcl5, Cxcl7 and Cxcl15 in tumor tissue from *Pf4-Cre-* and *Pf4-Cre+* mice. Expression levels of (A) Cxcl3, (B) Cxcl5, (C) Cxcl7 and (D) Cxcl15 (relative to β2-microglobulin) in RT2 tumor tissue were not significantly different between *Pf4-Cre-* (n=7) and *Pf4-Cre+* (n=4) mice (Cxcl3: *P*=0.7879; Cxcl5: *P*=0.9273; Cxcl7: *P*=0.4121; Cxcl15; *P*=0.3152).